Current Applied Physics 13 (2013) 1490–1495

Contents lists available at SciVerse ScienceDirect

Current Applied Physics

journal homepage: www.elsevier.com/locate/cap

Structural and dielectric properties of polyvinyl alcohol/barium zirconium titanate polymer–ceramic composite

T. Badapanda [a,*], V. Senthil [a], S. Anwar [b], L.S. Cavalcante [c], N.C. Batista [c], E. Longo [d]

[a] Department of Physics, CV Raman College of Engineering Bhubaneswar, Rourkela, Orissa 752054, India
[b] Colloids & Materials Chemistry, CSIR-Institute of Minerals and Materials Technology, Bhubaneswar 751013, India
[c] UESPI, CCN, Departamento de Química, Rua João Cabral, P.O. Box 2231, 64002-150 Teresina, PI, Brazil
[d] Universidade Estadual Paulista, P.O. Box 355, 14801-907 Araraquara, SP, Brazil

ARTICLE INFO

Article history:
Received 17 January 2013
Received in revised form
26 April 2013
Accepted 5 May 2013
Available online 28 May 2013

Keywords:
Polymer-matrix composites
Rietveld refinement
Clusters
Dielectric properties

ABSTRACT

The polyvinyl alcohol (PVA)/barium zirconium titanate $Ba[Zr_{0.1}Ti_{0.9}]O_3$ (BZT) polymer–ceramic composites with different volume percentage are obtained from solution mixing and hot-pressing method. Their structural and electrical properties are characterized by X-ray diffraction (XRD), Rietveld refinement, cluster modeling, scanning electron microscope and dielectric study. XRD patterns of PVA/BZT polymer–ceramics composite (with 50% volume fractions) indicate no obvious differences than the XRD patterns of pure BZT which shows that the crystal structure is still stable in the composite. The scanning electron micrograph indicates that the BZT ceramic is dispersed homogeneously in the polymer matrix without agglomeration. The dielectric permittivity (ε_r) and the dielectric loss ($\tan\delta$) of the composites increase with the increase of the volume fraction of BZT ceramic. Theoretical models are employed to rationalize the dielectric behavior of the polymer composites. The dielectric properties of the composites display good stability within a wide range of temperature and frequency. The excellent dielectric properties of these polymer–ceramic composites indicate that the BZT/PVA composites can be a candidate for embedded capacitors.

1. Introduction

Recently there has been a constant search for new materials that possess high dielectric permittivity and good mechanical properties for important technological applications. Polymers are materials with low-density flexible, easy to fabricate and superior in dielectric breakdown strength and mechanically more compliant than the ceramics, but its dielectric values are much lower than those of the ceramics [1]. On the other hand, ferroelectric ceramics possess high dielectric permittivity, but with poor mechanical properties and lower dielectric breakdown strength [2]. By integrating high dielectric permittivity ceramic powder with superior dielectric strength of the polymer, it is possible to develop a composite with high dielectric permittivity and high breakdown strength [3–10]. This type of composites has high capability of energy storage and can be used in capacitors and energy storage devices [11]. The easiness of composite fabrication allows producing thin film capacitors which are difficult to achieve with ceramics due to complicated fabrication routes.

Polyvinyl alcohol (PVA) is a good insulating material with low conductivity, hence it is very useful in microelectronic industry [12]. It's electrical conductivity depends on the thermally generated carriers and also with the addition of suitable dopants. Moreover, the PVA polymer extends the industrial applications in optical, pharmaceutical, medical, and membrane fields. PVA is a semi-crystalline material with several interesting physical properties, which are very useful in technical applications [13]. Different additives have been added in PVA to modify and improve its dielectric properties [14]. Inorganic additives, such as: transition metal salts have a considerable effect on the optical and electrical properties of PVA polymer [15].

The perovskite family of ferroelectric materials is used in the fabrication of various devices like sensors, actuators, transducers, capacitors, etc., which are widely used in many electronic components of the modern world [16,17]. Barium zirconium titanate $Ba[Zr_{0.1}Ti_{0.9}]O_3$ (BZT) ceramic has attracted immense attention for its potential applications for the microwave technology and piezoelectric devices, due to their high dielectric constant, low dielectric loss, and large tunability because the substitution of Zr^{4+} for Ti^{4+} ions has a benefit to the stability of the system [18,19].

* Corresponding author. Tel.: +91 94 37306100, +91 06 612462999 (mobile).
E-mail address: badapanda.tanmaya@gmail.com (T. Badapanda).

1567-1739/$ – see front matter © 2013 Elsevier B.V. All rights reserved.
http://dx.doi.org/10.1016/j.cap.2013.05.006

Therefore, in this work, we report on the structure, cluster modeling and dielectric study of BZT/PVA polymer–ceramic composites with various BZT volume fractions fabricated by a solution mixing and hot-pressing process.

2. Experimental details

BZT ceramic was prepared by the solid state reaction method. Barium carbonate ($BaCO_3$) Merck-Germany (99.5% purity), titanium oxide (TiO_2) Merck-Germany (99% purity) and zirconium oxide (ZrO_2) Merck-Germany (99% purity) were used as precursors. The PVA have a molecular weight ≈14,000 with glass transition temperature at around 70 °C and melting point 220 °C was used as a polymer matrix. All the precursors were measured stoichiometrically and ball milled for 12 h, followed by heat treatment at 1350° for 4 h. The ceramic powder was characterized by the X-ray diffraction (XRD) in a PANalytical X-ray diffractometer (Netherlands). Polymer–ceramic composites were prepared by mixing of the synthesized BZT ceramic with the PVA polymer at different volume percentage (10, 20, 30, 40, and, 50%) in the aqueous solution of PVA. These composites were dried by using an infrared lamp and hot pressed at 100 °C for 5 min using the pressure 300 MPa. The microstructure of PVA/BZT composites was investigated by the scanning electron microscope, model JEOL (USA). For electrical measurements the hot pressed discs were coated with silver metallic paste on both sides of the thick films. Frequency and temperature dependence of the electrical properties were measured using N4L-NumetriQ (model PSM1735) connected to PC with the rising temperature of 1.2 °C/min from 30 °C to 150 °C.

3. Results and discussion

3.1. XRD patterns and Rietveld refinement analyses

To investigate the crystal structure and effect of BZT ceramic in the PVA polymer matrix the XRD patterns were performed. Fig. 1(a) illustrates the XRD patterns of pure PVA polymer, BZT ceramics and BZT/PVA ceramics/polymer composites (50/50), and Fig. 1(b) shows the Rietveld refinement plot of BZT ceramics heat-treated at 1350 °C for 4 h, respectively.

XRD pattern of pure PVA polymer indicates a broad peak at 22° which is attributed to non-crystalline or amorphous behavior of the polymer corresponding to the structural disorder at long range, in agreement with the literature [20]. The XRD pattern to BZT ceramic indicates that this material presents a single phase with tetragonal structure. Moreover, the XRD pattern of PVA/BZT polymer–ceramics composite (with 50% volume fractions) indicates no obvious differences than the XRD patterns of pure BZT which indicates that the crystal tetragonal structure of BZT is still stable in the composite (Fig. 1(a)). It can also be interpreted from these XRD patterns that there is no undesired interaction at the interface of PVA–BZT upon dispersion in PVA. Rietveld refinement plot illustrated in Fig. 1(b), indicates that BZT ceramic has a perovskite-type tetragonal structure with a space group (*P4mm*) [21]. All the diffraction peaks are in good agreement with the respective Inorganic Crystal Structure Database (ICSD) card N°. 100802 [21]. The Rietveld analysis indicates that the BZT ceramic is highly crystalline. Moreover, Fig. 1(b) shows a good agreement between the observed XRD patterns and the theoretical fitting results. The fit parameters (R_{wnb}, R_b, R_{exp}, R_w and σ) suggest that the refinement results are very reliable. Finally, we have employed the structural parameters listed in Table 1 to model the supercells (1 × 5 × 2) of BZT ceramic by means of the visualization for electronic and structural analysis (VESTA) software (Version 3.1.1 for Windows).

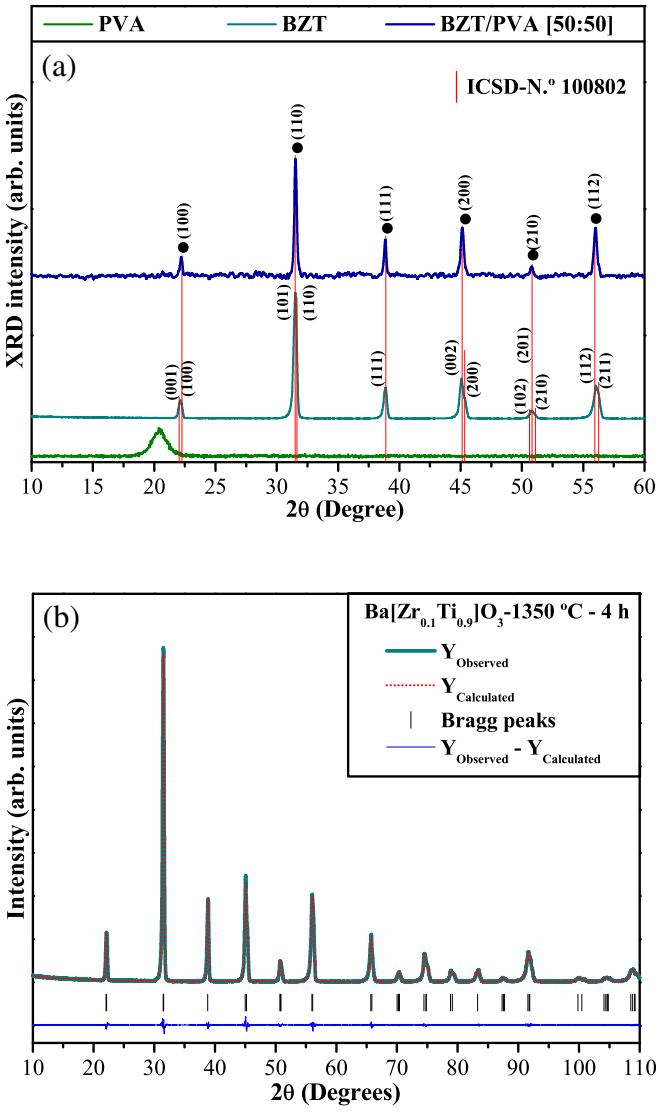

Fig. 1. (a) X-ray diffraction pattern for the hot-pressed PVA, BZT and (b) PVA + 50 vol.% BZT. (b) Rietveld refinement plots of BZT ceramic.

3.2. Representation for the $Ba[Zr_{0.1}Ti_{0.9}]O_3$ lattice and PVA polymer matrix

Fig. 2(a, b) shows the representations for the BZT supercells and molecular structure of PVA polymer, respectively.

Fig. 2(a) illustrates the supercells (1 × 5 × 2) for BZT ceramics with tetragonal structure, space group (*P4mm*) and point-group symmetry (O_h). In this supercells, the zirconium (Zr) and titanium

Table 1
Lattice parameters, unit cell volume, *c*/*a* ratio and atomic positions for the Ba$[Zr_{0.1}Ti_{0.9}]O_3$ heat-treated at 1350 °C for 4 h.

Atoms	Wyckoff	Site	*x*	*y*	*z*	Occupancy
Ba	1*a*	4*mm*	0	0	0	1
Zr	1*b*	4*mm*	0.5	0.5	0.50	0.1
Ti	1*b*	4*mm*	0.5	0.5	0.48855	0.9
O1	1*b*	4*mm*	0.5	0.5	−0.02013	1
O2	2*c*	2*mm*	0.5	0	0.48921	1

P4mm (99) – tetragonal ($a = b = 4.0068$ Å; $c = 4.0242$ Å; $c/a = 1.0043$; $V = 64.67$ Å^3). $R_w = 6.354\%$; $R_{wnb} = 5.845\%$; $R_b = 4.5841\%$; $R_{exp} = 2.854\%$ and $\sigma = 2.226$.

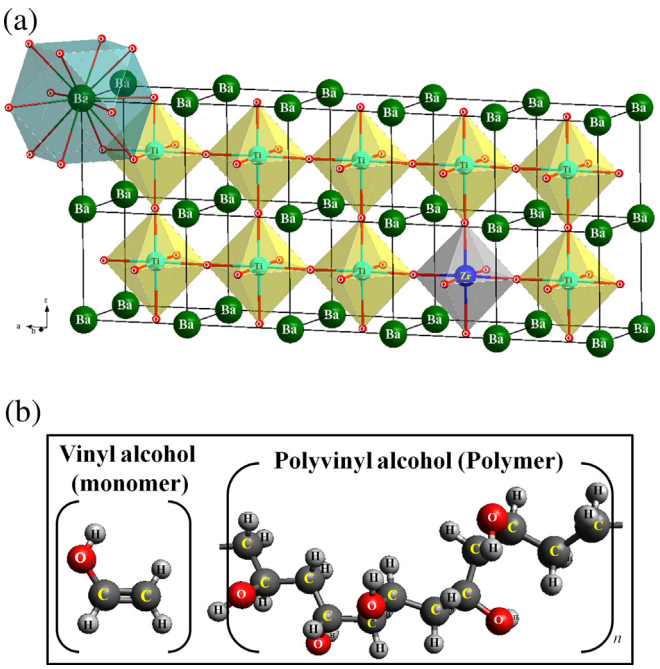

Fig. 2. (a) BZT supercells (1 × 5 × 2) and (b) molecular structure of PVA polymer.

(Ti) atoms are coordinated to six oxygen (O) atoms forming to octahedral $[TiO_6]/[ZrO_6]$ clusters. Moreover, we can observe that the barium (Ba) atoms are coordinated to twelve O atoms forming the cuboctahedral $[BaO_{12}]$ clusters. The cuboctahedron presents twelve identical vertices, formed by the meeting of two triangles and two squares, fourteen faces and twenty-four identical edges, each separating a triangle from a square [22]. The structure molecular of PVA polymer is formed by several units of vinyl alcohol (VA) or ethanol molecule (Fig. 2(b)). The PVA is indirectly formed by the polymerization process of vinyl acetate followed by the formation of water molecules (H_2O) or hydrolysis of the ester bonds and finally has the formation of PVA polymer and acetic acid (HOAc) as products, according to the reactions by Equations (1) and (2) below:

$$n\ldots(CH_2{=}CHOAc) \xrightarrow{\Delta} (CH_2{=}CHOAc)_n, \quad (1)$$

$$(CH_2{=}CHOAc)_n + n\cdot H_2O \xrightarrow{\Delta} (CH_2{-}CHOAc)_n + n\cdot HOAc. \quad (2)$$

The representation of the molecular structure of VA monomer and PVA polymer matrix employed in preparation of PVA/BZT polymer–ceramic composites is shown in Fig. 2(b).

3.3. Microstructural analyses

Fig. 3(a–f) illustrates the SEM images of surface for the pure PVA polymer and PVA/BZT ceramic/polymer composites, respectively.

Fig. 3(a) shows a uniform surface for PVA polymer, while the BZT/PVA ceramics/polymer composites shown the presence of fine grain related to BZT ceramics merged into the PVA polymer matrix Fig. 3(b–f). Moreover, SEM image of pure PVA polymer exhibits no features attributable to any crystalline morphology. The raise in the roughness degree with increased ceramic concentration indicates the segregation of the dopant in the host matrix. Therefore, the microstructure of BZT/PVA ceramics/polymer composites illustrated by SEM images (Fig. 3(b–f)) indicates clearly the presences of BZT grains with surface roughness in light region are more dense and compacted while the dark region are related to PVA polymer with a smooth surface. The uniformity of the white dots indicates that the BZT are homogenously dispersed in the PVA polymer.

3.4. Dielectrics properties analyses

Fig. 4(a, b) illustrates the variation of relative dielectric permittivity (ε_r)/dielectric loss (tan δ) in relation to frequency (kHz) and ε_r values for BZT/PVA ceramics/polymer composites with different relation in volume (%) sintered at 1200 °C for 2 h, respectively.

Fig. 4(a) shows the variation of ε_r with frequency at room temperature for PVA/BZT polymer–ceramic composites. The low frequency dispersion rises with the increase of the BZT content in PVA/BZT composites. The reason for the increase of dielectric constant at low frequency dispersion can be due to the space charge effects [23]. The dielectric constant decreases with increase in frequency may be due to the dielectric relaxation of the BZT ceramics and the interfaces in the composite. Dielectric relaxation could originate from the alternations of the elastic and electric behavior and the movement of the domain walls in high frequency regions [24]. The variations of loss tangent with frequency for the PVA/BZT polymer–ceramic composites are shown in Fig. 4(b). It was found that the tan δ increases gradually with the increase of BZT content. As shown in Fig. 4(b), the tan δ values are found to be decreasing with increasing frequency which may be due to the fall in electrical conductivity of the composites with increasing frequency. It can also be noticed that the frequency dependencies of dielectric constant and loss tangent rise with increasing ceramic loading. The increase in dielectric constant and loss tangent with increasing BZT content could be interpreted as interface charge polarization and intrinsic electric dipole polarization inside the composites in applied alternating fields [25,26]. This phenomenon appears in the heterogeneous system like PVA/BZT polymer–ceramic composites due to the accumulation of electric charges at the interface boundaries and the formation of large dipoles on ceramic particles or clusters. In the present case, the degree of polarization inside the composite system increases with the increase in particle concentration, which in turn enhances the dielectric constant of polymer–ceramic composites.

As shown in Fig. 4(a), the dielectric constant gradually increases with increasing temperature. The increase in dielectric property in the composites may be due the two mechanisms: (I) the segmental mobility of polymer would improve with increasing temperature, which should facilitate the polarization of polar components and increase the dielectric constant consequently, and (II) the structure of BZT grains could be changed with an increase in temperature (before Curie temperature), which could generate a modification on the dielectric response of the ceramic. But the rise in dielectric constant with rise in temperature decreases with increase in frequency as shown in Fig. 4(a). There is no significant change in the dielectric constant in the 100 kHz–1 MHz frequency range even at high temperature. The dielectric loss (Fig. 4(b)) also increases as the temperature increases and decreases as the frequency increases.

It also can be seen in Fig. 5(a) that there is a strong dispersion in dielectric constant at low frequencies and it merges at high frequencies. This explains that the dielectric behavior of polymer ceramic composites is frequency dependent, which is the typical nature of ferroelectric/ceramic materials. It is also observed that the permittivity decreases monotonically with increasing frequency and attains a constant value at higher frequencies. The modified Debye equation related to free dipole oscillating in an alternating field is expressed in Equation (3):

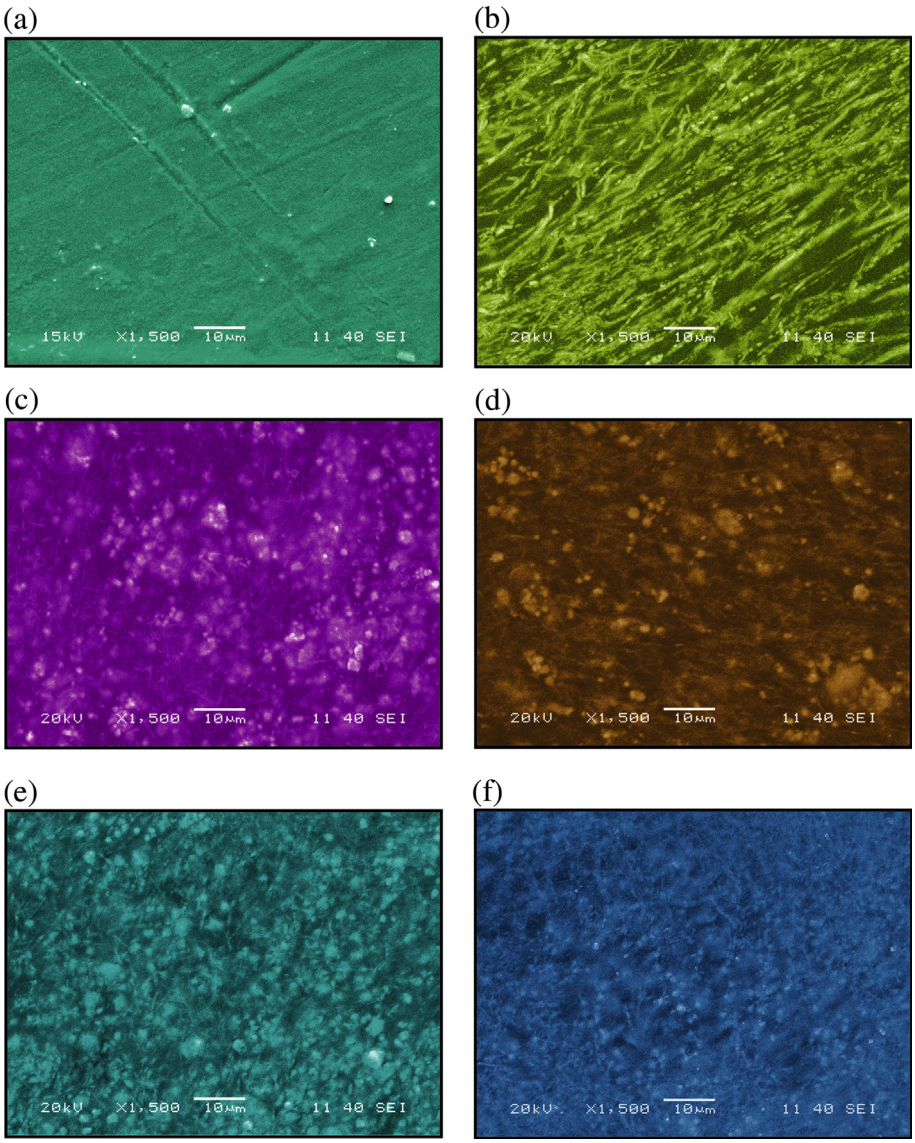

Fig. 3. SEM image of (a) pure PVA, (b) PVA + 10% BZT, (c) PVA + 20% BZT, (d) PVA + 30% BZT, (e) PVA + 40% BZT, (f) PVA + 50% BZT.

$$\varepsilon^* = \varepsilon' - i\varepsilon'' = \varepsilon_\infty + \frac{\varepsilon_s - \varepsilon_\infty}{1 + (i\omega\tau)^{1-\alpha}}, \quad (3)$$

where, ε_s and ε_∞ are the low and high frequency values of ε', $\omega = 2\pi f$, f is being the frequency of measurement, τ is the relaxation time, and α is a measure of distribution of relaxation time. At very low frequencies dipoles follow the field and we have $\varepsilon' \approx \varepsilon_s$ whereas with the increase of frequency ($\omega < 1/\tau$), dipoles lag behind the field and ε' starts decreasing. When the frequency reaches the characteristic frequency ($\omega = 1/\tau$), the dielectric constant drops. At very high frequencies, dipoles can no longer follow the field and $\varepsilon' \approx \varepsilon_\infty$, also there exists polarization effect. The low-frequency dispersion region is attributed to charge accumulation at the electrode–electrolyte interface. At higher frequencies, the periodic reversal of the electric field occurs quickly that there is no excess ion diffusion in the direction of the field. Hence, the relative dielectric permittivity referent to imaginary (ε'_r) decreases with increasing frequency in the PVA/BZT composites. In Fig. 5(b) is presented the variation of tan δ of PVA/BZT composites (50:50) with respect to frequencies at different temperature. It indicates the presence of temperature dependent relaxation in the composites. The relaxation peak shifts to the high frequency side with an increase in temperature. A small hike appears in composites which indicate the activated space charge polarization at low frequencies and thus acts as a dipole. It also indicates the presence of one more relaxation mechanism due to the hopping frequency of charge carriers which coincides with that of external field [27]. By addition of BZT in the polymer matrix, more and more free charges may accumulate on the interface resulting in a decrease of relaxation time and thus, the relaxation process shifts toward the higher frequencies [28].

In the present work, various models are used in order to predict the effective dielectric constant of the composite. Fig. 6 shows the room temperature dielectric constant of the composite at 1 kHz (experimental) and the dielectric constant calculated based on various models for different volume fractions of BZT. There are a number of models to predict the effective dielectric constant of the composites. In the present study the following equations were used to calculate the effective relative permittivity of the PVA/BZT composites. The dielectric property of a biphasic dielectric mixture comprising of spherical crystallites with high dielectric constant dispersed in a matrix of low

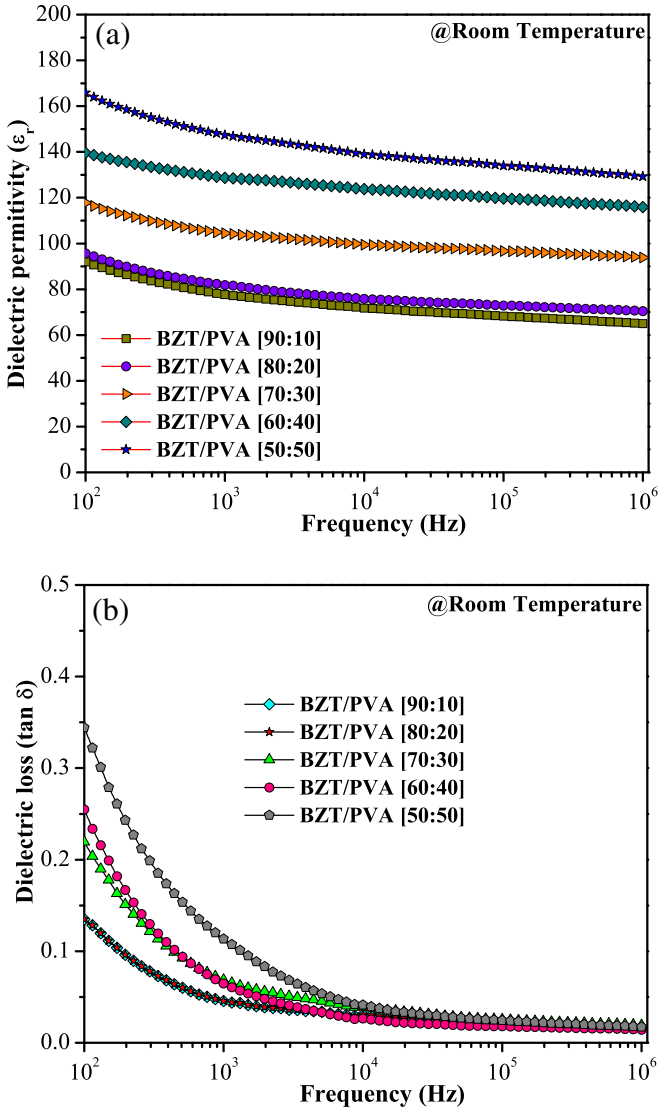

Fig. 4. Frequency dependence of (a) dielectric constant and (b) dielectric loss at room temperature of PVA/BZT composite as a function of volume percent of BZT.

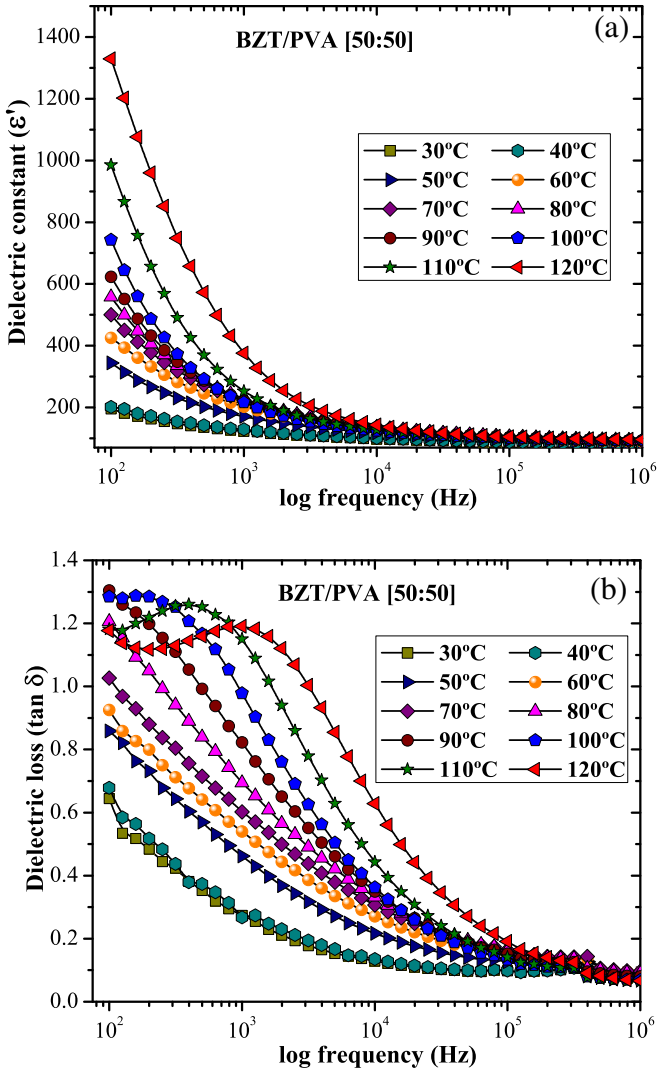

Fig. 5. Frequency dependent (a) dielectric constant and (b) dielectric loss for PVA + 50 vol.% BZT composite at different temperatures.

dielectric constant could be well described by Maxwell's model [29] as presented in Equation (4):

$$\varepsilon_{\text{eff}} = \left(\frac{\delta_p \varepsilon_p \left(\frac{2}{3} + \varepsilon_c / 3\varepsilon_p \right) + \delta_c \varepsilon_c}{\delta_p \left(\frac{2}{3} + \varepsilon_c / 3\varepsilon_p \right) + \delta_c} \right), \tag{4}$$

where, ε_c, ε_p, δ_c, and δ_p are the dielectric constants of ceramic, polymer, the volume fraction of the ceramic and the polymer, respectively.

The most commonly used dielectric mixture rule is Lichtenecker's [30], which is also referred to as the logarithmic mixture rule in Equation (5).

$$\log \varepsilon_{\text{eff}} = \delta_1 \log \varepsilon_p + \delta_1 \log \varepsilon_c. \tag{5}$$

The effective medium theory (EMT) model [31] has been established taking into account the morphology of the particles. According to which the effective dielectric constant is given by Equation (6):

$$\varepsilon_{\text{eff}} = \varepsilon_p \left[1 + \frac{f_c(\varepsilon_c - \varepsilon_p)}{\varepsilon_p + n(1 - f_c)(\varepsilon_c - \varepsilon_p)} \right], \tag{6}$$

where, f_c is the volume fraction of the ceramic dispersed, and n is the ceramic morphology fitting factor respectively. The small value of n indicates the filler particles to be in near-spherical shape, while a high value of n indicates largely non-spherically shaped particles. The theoretical morphology fitting factor is closer to that of the experimental one, and is consistent with that observed (irregular shaped particles) in the present studies (Fig. 3(a–f)). A close agreement is found between the experimental and theoretical values which are achieved with n equal to 0.45.

According to Yamada et al. [32], the effective dielectric constant can be expressed in Equation (7) below:

$$\varepsilon_{\text{eff}} = \varepsilon_p \left[1 + \frac{n \cdot f_c(\varepsilon_c - \varepsilon_p)}{n \cdot \varepsilon_p + n(1 - f_c)(\varepsilon_c - \varepsilon_p)} \right], \tag{7}$$

where, n is the parameter related to the geometry of the ceramic particles. The parameter n is evaluated to fit the theoretical value obtained from Equation (6) to the observed values. The

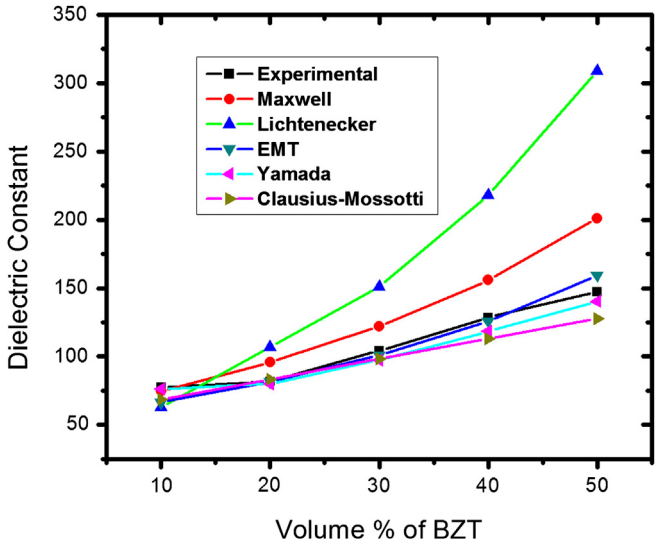

Fig. 6. Variation of effective dielectric constant measured at room temperature and 1 kHz of PVA/BZT composite as a function of volume percent of BZT ceramic and comparison with calculated value by using various models.

experimental results are comparable to the calculated value using this model, when the parameter n is around 0.7.

The Clausius–Mossotti model [33] was also used for predicting the effective dielectric constant of a mixture composed of spherical crystallite dispersed in a continuous medium. The effective dielectric constant (ε_{eff}) of the composite is calculated using the Equation (8):

$$\varepsilon_{eff} = \varepsilon_p \left[1 + 3\delta_c \left(\frac{(\varepsilon_{c-\varepsilon_p})}{(\varepsilon_c + 2\varepsilon_p)} \right) \right]. \quad (8)$$

Among the various models used for rationalizing the dielectric behavior, experimental ε_{eff} at different volume fractions is comparable with those obtained with the models like EMT ($n = 0.45$) and Yamada ($n = 0.7$).

4. Conclusions

In summary, the BZT ceramic and PVA/BZT polymer–ceramic composites were obtained by the solid state reaction method (1350 °C for 4 h) by the solvent mixing and hot pressing. The XRD pattern of PVA polymer showed the presence of orthorhombic structure. The XRD patterns and Rietveld refinement analysis of BZT ceramic showed a perovskite-type tetragonal structure. Rietveld refinement data were employed to model [BaO_{12}], [ZrO_6], and [TiO_6] clusters by lattice parameters and atomic positions. The SEM images showed that there is no agglomeration and good distribution of BZT ceramic within the PVA polymer matrix. The dielectric study revealed that the dielectric constant and dielectric loss increases with the increase in ceramic content. The PVA/BZT polymer–ceramic composite (50:50) showed frequency and temperature dependence dielectric behavior. Although the dielectric constant increases with increasing temperature, the rise in dielectric constant with rise in temperature is not significant at frequencies from 10 kHz to 1 MHz. The high dielectric constant, low loss tangent and stable dielectric properties make the PVA/BZT polymer–ceramic composites as a good candidate material for various industrial applications.

Acknowledgments

The Brazilian authors acknowledge the financial support of the Brazilian research financing institutions: CNPq (350711/2012-7), CNPq-GERATEC (555684/2009-1), and CAPES. Special thanks to Professor Dr. Tanmaya Badapanda for consolidating the partnership of this research between India and Brazil.

References

[1] Y. Liu, K.L. Ren, H.F. Hofmann, Q. Zhang, IEEE Trans. Ultrason. Ferroelectr. Freq. Control 52 (2005) 2411–2417.
[2] Y. Song, Y. Shen, H. Liu, Y. Lin, M. Li, C.-W. Nan, J. Mater. Chem. 22 (2012) 8063–8068.
[3] G.H. Haertling, J. Am. Ceram. Soc. 82 (1999) 797–818.
[4] D.-H. Kuo, C.-C. Chang, T.-Y. Su, W.-K. Wang, B.-Y. Lin, Mater. Chem. Phys. 85 (2004) 201–206.
[5] B. Hilczer, J. Kulek, E. Markiewicz, M. Kosec, Ferroelectrics 293 (2003) 253–265.
[6] C. Huber, M. Treguer-Delapierre, C. Elissalde, F. Weill, M. Maglione, Ferroelectrics 294 (2003) 13–24.
[7] K. Li, G. Pang, H.L.W. Chan, C.L. Choy, J.-H. Li, J. Appl. Phys. 95 (2004) 5691–5696.
[8] B. Hilczer, J. Kulek, E. Markiewicz, M. Kosec, Ferroelectrics 267 (2002) 279–288.
[9] D.-N. Fang, A.K. Soh, C.-Q. Li, B. Jiang, J. Mater. Sci. 36 (2001) 5281–5288.
[10] C.E. Ciomaga, R. Calderone, M.T. Buscaglia, M. Viviani, V. Buscaglia, L. Mitoseriu, A. Stancu, P. Nanni, J. Optoelectron. Adv. Mater. 8 (2006) 944–948.
[11] P. Muralt, J. Micromech. Microeng. 10 (2000) 136–146.
[12] H.M. Zidan, J. Appl. Polym. Sci. 88 (2003) 104–108.
[13] A.L. Saroj, R.K. Singh, Phase Trans. 84 (2011) 231–242.
[14] Z. Wang, J.K. Nelson, J. Miao, R.J. Linhardt, L.S. Schadler, IEEE Trans. Dielectr. Electr. Insul. 19 (2012) 960–967.
[15] D.K. Das-Gupta, S. Zhang, Ferroelectrics 134 (1992) 71–77.
[16] P.W. Rehrig, S.E. Park, S. Trolier-MsKinstry, G.L. Messing, B. Jones, T.R. Shrout, J. Appl. Phys. 86 (1999) 1657–1662.
[17] U. Weber, G. Greuel, U. Boettger, S. Weber, D. Hennings, R. Waser, J. Am. Ceram. Soc. 84 (2001) 759–766.
[18] N. Cramer, E. Philofsky, L. Kammerdiner, T.S. Kalkur, Appl. Phys. Lett. 84 (2004) 771–773.
[19] Z. Yu, C. Ang, R. Guo, A.S. Bhalla, J. Appl. Phys. 92 (2002) 1489–1493.
[20] R. Wäesche, W. Denner, H. Schulz, Mater. Res. Bull. 16 (1981) 497–500.
[21] F. Moura, A.Z. Simões, E.C. Aguiar, I.C. Nogueira, M.A. Zaghete, J.A. Varela, E. Longo, J. Alloys Compd. 479 (2009) 280–283.
[22] S.M. Reddy, S.S. Rao, N. Venkanna, K.N. Reddy, Int. J. Chem. Anal. Sci. 2 (2011) 126–129.
[23] W.X. Yuan, Z.J. Li, J. Phys. Chem. Solids 73 (2012) 599–603.
[24] J.E. Garcia, R. Perez, A. Albareda, J. Phys. D Appl. Phys. 34 (2001) 3279–3284.
[25] H.T. Vo, F.G. Shi, J. Microelectron. 33 (2002) 409–415.
[26] G.C. Psarras, E. Manolakaki, G.M. Tsangaris, Compos. Part A 33 (2002) 375–384.
[27] S. Sumi, P. Rao, M. Deepa, P. Koshy, J. Appl. Phys. 108 (2010) 063718–063726.
[28] G. Chakraborty, A.K. Meikap, R. Babu, W.J. Blau, Solid State Commun. 151 (2011) 754–758.
[29] J.C. Maxwell, A Treatise on Electricity and Magnetism, Dover Publ. Co., New York, 1954.
[30] H.S. Nalwa, Ferroelectric Polymers, Marcel Dekker, New York, 1995. (Chapter 11).
[31] Y. Rao, J. Qu, T. Marinis, C.P. Wong, IEEE Trans. Compon. Packag. Technol. 23 (2000) 680–683.
[32] T. Yamada, T. Ueda, T. Kitayama, J. Appl. Phys. 53 (1982) 4328–4332.
[33] H. Frolich, Theory of Dielectrics, Clarendon Press, Oxford, 1949.